ELSEVIER DEVELOPMENTS IN VOLCANOLOGY 7

THE SOUTH AEGEAN ACTIVE VOLCANIC ARC

PRESENT KNOWLEDGE AND FUTURE PERSPECTIVES

EDITED BY
M. FYTIKAS AND G.E. VOUGIOUKALAKIS

THE SOUTH AEGEAN ACTIVE VOLCANIC ARC

Edited by
Fytikas

Included in series
Developments in Volcanology.

Contents
1. Tertiary and Queternary tectonics in the Aegean area (D. Mountrakis). 2. A model of the Aegean geodynamic zone (B. Ranguelov). 3. Upper mantle structure of the Aegean (Greece) derived from phase velocities of fundamental mode Rayleigh waves (I. Kassaras, K. Makropoulos). 4. Deep structure and active tectonics of the Southern Aegean volcanic arc (B.C. Papazachos *et al.*). 5. A west-east traverse along the magmatism of the South Aegean volcanic arc in the light of volcanological, chemical and isotope data (L. Francalanci *et al.*). 6. The South Aegean active volcanic arc: relationships between magmatism and tectonics (G. Pe-Piper, D.J.W. Piper). 7. Our bubbling earth (R.D. Schuiling). 8. Magmatic evolution processes as recorded in plagioclase phenocrysts of Nea Kameni rocks (Santorini volcano, Greece) (A.P. Santo). 9. Volcanic hazards in the Aegean area, relative risk evaluation and monitoring state of the active volcanic centers (G.E. Vougioukalakis, M. Fytikas). 10. Recent seismic activity (1994-2002) of the Santorini volcano using data from local seismological network (I.M. Dimitriadis *et al.*). 11. Geodetic evidence for slow, small scale inflation of the Santorini caldera (S.C. Stiros, A. Chasapis, V. Kontogianni). 12. Long-term prediction of the next eruption in Thera volcano from conditional probability estimates (G.A. Papadopoulos, K. Orfanogiannaki). 13. Late-Holocene coastal uplift in the Nisyros volcano (SE Aegean Sea): Evidence for a probable new phase of slow shallow intrusive activity (S.C. Stiros*et al.*). 14. Investigating the formation of a superficial fracture on Nisyros Island, Greece with the DC resistivity method (D. Galanopoulos, G. Kolettis). 15. Gravity monitoring of Nisyros volcano activity: 2001-2003 preliminary results (M. Di Filippo, B. Toro). 16. Real time monitoring of gas-geochemical parameters in Nisyros fumaroles (M. Teschner *et al.*). 17. The Vani manganese deposit, Milos island, Greece: A fossil stratabound Mn-Ba-Pb-Zn-As-Sb-W-rich hydrothermal deposit (G.P. Glasby *et al.*). 18. An FT-Raman, Raman and FTIR study of hydrothermally altered volcanic rocks from Kos Island (Southeastern Aegean, Greece) (D. Papoulis *et al.*). 19. Rhyolitic dikes of Paros Island, Cyclades (A. Hannappel, T. Reischmann). 20. Investigation of non-pristine volcanic structures acting as probable hosts to epithermal gold mineralization in the back arc region of the active Aegean Arc, used combined satellite imagery and field data: examples from Lesvos volcanic terrain (C. Vamvoukakis*et al.*). 21. Tertiary high-Mg volcanic rocks from Western Anatolia and their geodynamic significance for the evolution of the Aegean area (S. Agostini *et al.*). 22. A mathematical model for the morphological evolution of a volcano on an island (G.A. Skianis, D. Vaiopoulos, V. Tsarbos).

Bibliographic & ordering Information
Hardbound, ISBN: , publication date: 2004
Imprint: ELSEVIER

DEEP STRUCTURE AND ACTIVE TECTONICS OF THE SOUTHERN AEGEAN VOLCANIC ARC

B. C. Papazachos[1], S. T. Dimitriadis[2], D. G. Panagiotopoulos[1], C. B. Papazachos[1] and E. E. Papadimitriou[1]

[1] Geophysical Laboratory, Dept. of Geophysics, School of Geology, Aristotle University of Thessaloniki, P.O. Box 352-1, GR-54124 Thessaloniki, Greece

[2] Department of Mineralogy, Petrology and Economic Geology, School of Geology, Aristotle University of Thessaloniki, P.O. Box 352-1, GR-54124 Thessaloniki, Greece

Abstract

Data on spatial distribution of intermediate focal depth earthquakes, fault plane solutions and deep velocity structure have been used to further investigate active tectonics related to the deep structure of the southern Aegean volcanic arc. It is observed that the top layer of the subducted east Mediterranean lithospheric slab is seismically very active at depths 60 – 110km and 140 – 170km and that its low seismicity part (110 – 140km) is under the volcanic arc. This observation, geochemical data and tomographic results suggest that the primary magma reservoir of the Hellenic volcanic arc is in the mantle wedge between the subducted Mediterranean and the overriding Aegean slabs, at depths 60 – 90km. The genesis of earthquakes at the shallow part of the subducted Mediterranean slab is attributed to dehydration embrittlement of basalt, the low seismicity at intermediate depths is due to increase of temperature and confining pressure and the increase again of seismicity in the lower active part of the slab to a second dehydration embrittlement of hydrous eclogite.

Keywords: Aegean Sea, Volcanic arc, Active tectonics, Deep structure, Magma's genesis

Introduction

Southern Aegean is one of the most active tectonically regions of the whole western Eurasia. It is there where fast convergence of the Aegean microplate and the eastern Mediterranean lithosphere (front part of the African plate) occurs. The eastern Mediterranean lithosphere subducts under the Aegean and the Aegean microplate overrides the eastern Mediterranean (Papazachos and Comninakis, 1971; McKenzie, 1972). This physical process results in the generations: of shallow earthquakes with magnitudes up to 8.3 in the convergence boundary of the two plates (Hellenic trench), of intermediate focal depth earthquakes with magnitude up to 7.6 in the upper part of the subducted Mediterranean slab, and of shallow earthquakes with magnitudes up to 7.5 in the overriding Aegean microplate (Papazachos and Papazachou, 2003). It also results in the generation of volcanic activity along the Hellenic volcanic arc in southern Aegean (Georgalas, 1962; Fytikas et al, 1985).

Much work has been already done on active tectonics of the southern Aegean by the use of seismological data (Papazachos and Comninakis, 1969/70, 1971; McKenzie, 1970, 1978; Hatzfeld et al., 1989; Jackson, 1994) as well as of geodetic data (Straub and Kahle, 1994; LePichon et al., 1995; Reilinger et al., 1997; Papazachos, 1999; McClusky et al., 2000). However, some recent mainly seismological data can be used to better understand the deep structure and active tectonics in southern Aegean. Such data concern the spatial distribution of intermediate depth earthquakes, fault plane solutions, deep velocity structure and volcanic activity. For this reason, an attempt is made in the present work to use such data

for further studying of the active tectonics setting in the southern Aegean. Moreover, in this attempt we also focus on the processes definition of primary magma's genesis in southern Aegean and propose a model for that.

Spatial Distribution of Intermediate Depth Shocks

The spatial distribution of intermediate focal depth earthquakes in southern Aegean forms an amphitheatrical surface (Benioff zone) that dips from the convex to the concave part of the Hellenic arc. This zone was first identified by Papazachos and Comninakis (1969/70) and later investigated in detail (Papazachos and Comninakis, 1971; Hatzfeld et al., 1989; Papazachos et al., 2000). Additional new information is now available to better study the intermediate depth earthquakes in southern Aegean.

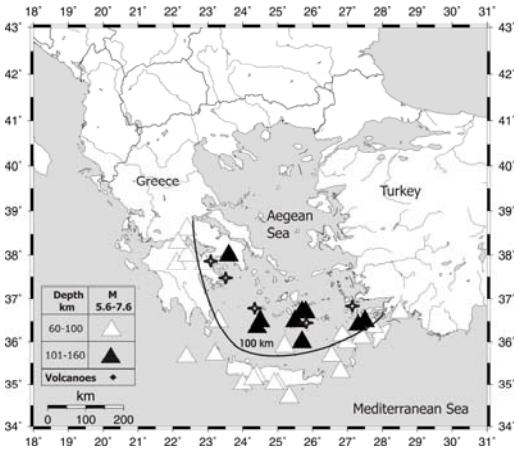

Fig. 1. Epicenters of strong intermediate depth earthquakes, which occurred in southern Aegean since 1911 (M≥6.0) and since 1965 (M≥5.6). White and black triangles denote depths smaller and larger than 100km, respectively. The isodepth of 100km and the five volcanic centers are also shown.

In the present work two complete samples of data for intermediate depth earthquakes in southern Aegean (34^0 N – 39^0 N, 20^0 E – 29^0 E) are used. The first sample includes 22 intermediate depth earthquakes (h = 60 – 155km) that have magnitudes M= 6.0 – 7.6 and occurred in the period 1911 – 1964 and the second sample includes 10 such earthquakes with M= 5.6 – 6.8 which occurred in the period 1965 – 2002. The parameters of these earthquakes are given in Papazachos et al. (2003). Figure (1) shows a map of the epicenters of these earthquakes which are denoted by open or solid triangles for earthquakes with focal depths 60 – 100km or 101 – 155km, respectively. In the same figure the isodepth of 100km and the five main volcanic centers are also shown. Figure (2) shows a plot of the distance, x (in km), of the epicenters from this isodepth of 100km (positive to the concave and negative to the convex part of the arc) as a function of the focal depth, h (in km). Least squares suggest a mean dip angle equal to ~25 degrees for x > 0.0km (depths >100km). Separate calculations for the western and eastern part of the arc give similar dip angles for the two parts, although tomographic profiles (Papazachos and Nolet, 1997) and spatial distribution of small recent shocks (Papazachos et al., 2000) show a steeper subduction for the eastern part of the slab and depths >100km. However, the dip angle gradually decreases for smaller depths (fig. 2) in agreement with previous results.

An interesting feature observed in figure (2) is the decrease of strong earthquake seismicity in the section of the subducted Mediterranean slab that is under the volcanic arc. To further test this observation, data for accurately located 104 intermediate depth shocks with magnitudes 4.0 – 6.3, which occurred in the southern Aegean in the period 1964 – 1979 (Comninakis and Papazachos, 1980) have been used. Figure (3) shows a plot of the frequency of shocks, n (percentage number of shocks per 10km depth), as a function of the focal depth.

This plot clearly shows a minimum of the frequency of shocks in the depth range of 110km – 140km. Based on the fact that both the sample of strong (M = 5.6 – 7.6) and the sample of smaller (M = 4.0 – 6.3) intermediate depth earthquakes in southern Aegean show a clear decrease of the frequency of shocks, as well as of the maximum magnitude (M_{max}= 6.7 in depths 110 – 140km), we may assume that this phenomenon is due to a change of the geophysical conditions in this part of the subducted oceanic crust. This change is discussed later in detail in conjunction with results from tomography and geochemical data.

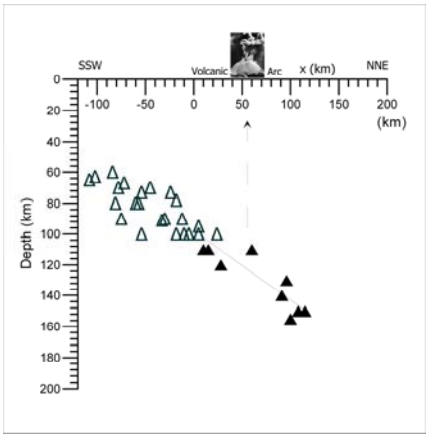

Fig. 2. Vertical profile of the Benioff seismic zone in southern Aegean as defined by the location of strong earthquakes (M ≥ 6.0 since 1911, M ≥ 5.6 since 1965)

The Stress Field

The orientation of the tectonic stress components and the corresponding faulting which are of interest for the present work are derived from fault plane solutions: a) of shallow earthquakes that occur in the southern Aegean volcanic arc, b) of shallow earthquakes that occur in the convex part of the Hellenic arc (Hellenic trench) where the Mediterranean and Aegean lithospheres converge and c) of intermediate depth earthquakes that are generated in the Benioff zone along the top oceanic crustal layer of the subducted Mediterranean slab. Such fault plane solutions have been published by several workers (Papazachos, 1961; McKenzie, 1972; Kiratzi and Langston, 1989; Taymaz et al., 1990; Papadimitriou, 1993, among many others). The most reliable of these solutions which concern strong (M≥5.5) earthquakes are included in a catalogue published by Papazachos and Papazachou (2003) that has been the source of relative data used in this work.

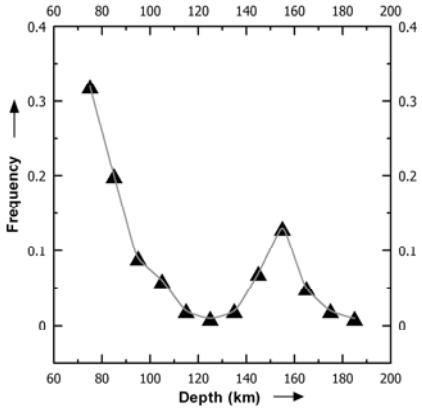

Fig. 3. Frequency, n, of intermediate depth shocks (M ≥ 4.0, per 10km depth) as a function of the focal depth (data for 104 accurately located shocks of the period 1964 – 1979, published by Comninakis and Papazachos (1980). A minimum for 110 – 140km focal depths is observed.

Reliable fault plane solutions for three strong shallow earthquakes (9.7.1956 M=7.5, 4.7.1968 M=5.5, 5.12.1968 M=6.0) in the volcanic arc are available. From these the representative solution has been derived by the method suggested by Papazachos and Kiratzi (1992) and is shown in the first line of table (1), where ζ, δ, λ are the strike, dip and rake of the representative fault and ξ and θ are the trend and plunge of the tensional axis. That is, the crust in the volcanic arc is dominated by a tensional field with a NW – SE direction which results in normal faults which strike NE – SW. Figure (4) shows the strikes of five such faults which are located in the five volcanic centers of the southern Aegean volcanic arc where a clustering of earthquake epicenters also occur (Papazachos and Panagiotopoulos, 1993).

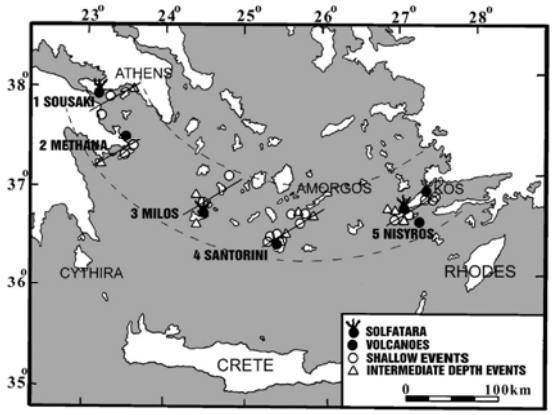

Fig. 4. The five seismovolcanic centers in the southern Aegean volcanic arc (after Papazachos and Panagiotopoulos, 1993).

A typical fault plane solution for the shallow earthquakes in the convex part of the Hellenic arc (Hellenic trench), where the Mediterranean and Aegean lithosphere converge, is shown in the second line of table (1) (Papazachos and Papazachou, 2003). That is, horizontal compression directed SSW – NNE dominates in the Hellenic trench, due to the convergence of the two plates in this direction. This results in the generation of shallow earthquakes (h < 60km) on low dip angle thrust faults, which strike NW – SE and dip NE.

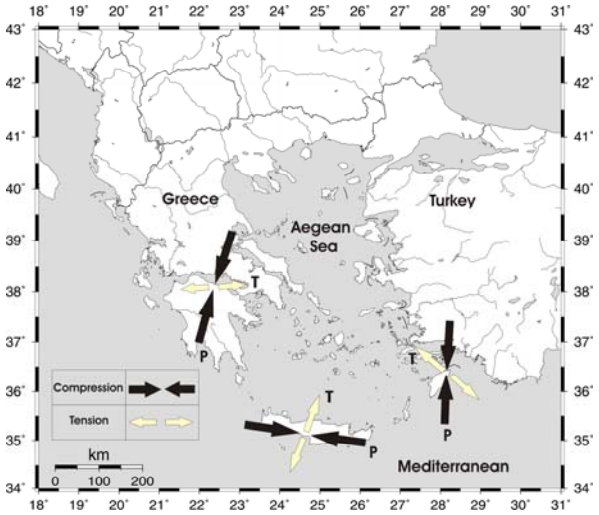

Fig. 5. Stress field in the shallow (60 – 110km) part of the subducted Mediterranean oceanic crust, beneath the western, central and eastern part of the Aegean.

Table 1. Parameters of the typical fault plane solutions for the shallow earthquakes in the volcanic arc and the Hellenic trench and for the intermediate focal depth earthquakes in the western, southern and eastern descending slab, respectively.

Region	**Fault Parameters**			**Tension**		**compression**	
	ζ	δ	λ	ξ	θ	ξ	θ
Volcanic Arc	231^0	40^0	-104^0	152^0	0^0	-	-
Hellenic Trench	309^0	23^0	101^0	211^0	23^0	-	-
W. Descending Slab	-	-	-	84^0	63^0	196^0	12^0
S. Descending Slab	-	-	-	20^0	49^0	279^0	9^0
E. Descending Slab	-	-	-	319^0	63^0	178^0	21^0

Reliable fault plane solutions are available for sixteen intermediate depth earthquakes that occurred in the shallower part (60 – 110km) of the descending oceanic crust. Four of these earthquakes occurred in the western part of the subducted slab and have typical solution shown in the third line of table (1). Eight of these earthquakes occurred in the central part of the descending slab and have a typical solution which is shown in the fourth line of table (1). The rest four of the earthquakes occurred in the eastern part of the slab and have a typical solution which is shown in the fifth line of table (1). Figure (5) shows on a map the horizontal projections of the P(compression) and of the T (tension) axes in the three parts of the slab. It is shown that the maximum tension is directed to the inner (concave) part of the arc and dips almost parallel to the dip direction of the descending Mediterranean slab, while the maximum compression is almost parallel to the strike of the arc, as it has been previously observed (Kiratzi and Papazachos, 1995). There are only two available fault plane solutions for the lower active part (140 – 180km) of the subducted slab, which also seem to show down-dip tension.

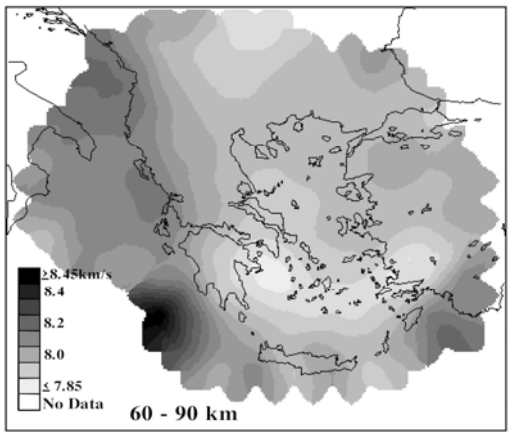

Fig. 6. P-velocity distribution at the depth of 60-90km in southern Aegean (Papazachos et al., 1995). A low velocity layer along the volcanic arc is clearly identified.

Deep Velocity Structure

Velocity structure concerns the crust and the upper part of the mantle where active tectonics take place. Information for such structure comes from recent seismic tomographic studies (Sapkman, 1986; Ligdas et al., 1990; Drakatos and Drakopoulos, 1991; Papazachos et al., 1995). Thus, such studies led to the conclusion that the subducted lithospheric eastern Mediterranean slab can be followed further to the north – northeast down to 600km or more (Spakman et al., 1988).

P-wave travel time tomography images of the crust and upper mantle for the depth range 60 – 90km show a clear low velocity layer along the volcanic arc of the southern Aegean, while no such layer is observed for depths 40 – 60km and 90 – 120km (Papazachos et al., 1995). This distribution is observed in fig. (6) where very low P velocities under the volcanic arc show that high temperature/partial melt material is found in this layer (60 – 90km). Since this layer lies directly under the volcanic arc, it may reasonably be concluded that this area corresponds to the primary magma source of the southern Aegean volcanic arc.

This idea is clearly supported by the results presented in figure (7), where three cross-sections in the west, central and eastern part of the subduction are shown. P-wave velocities are derived from the model of Papazachos and Nolet (1997) and the earthquakes of the western and eastern parts of the Benioff zone are superimposed on the corresponding tomographic images. In all sections we can easily identify the lack of strong earthquakes under the volcanic arc, as well as the low P-velocities at the depth of ~70-80km in the mantle wedge under the volcanic arc. This low velocity anomaly is less clear in the eastern section, however the corresponding mantle wedge velocities are still much lower than the corresponding slab velocities for the same depth range.

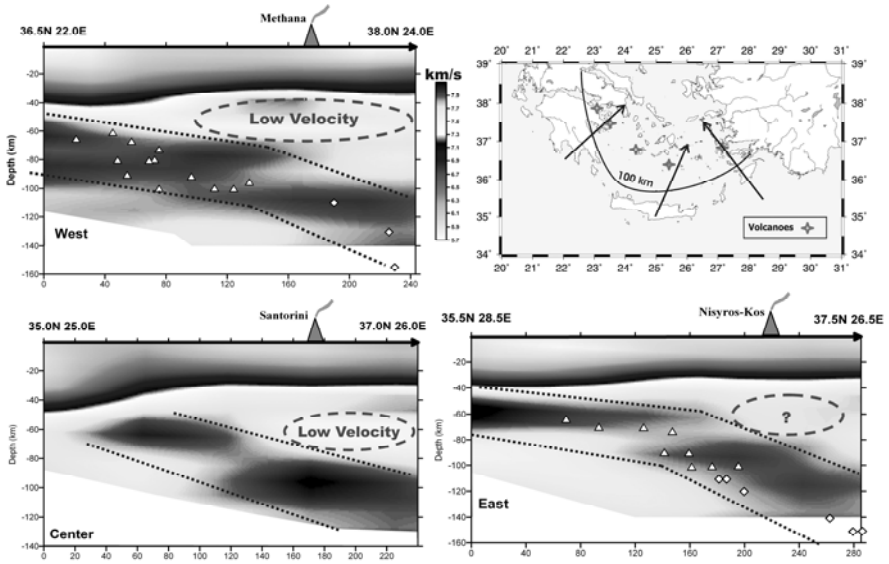

Fig. 7. P-velocity distribution along three cross-sections (west, central and east part) of the southern Aegean subduction, using the results of Papazachos and Nolet (1997). The intermediate depth seismicity of figure (2) is also superimposed for the western and eastern section of the slab. Notice the lack of seismicity in the Benioff zone and the low velocities in the mantle wedge under the volcanic arc.

Geochemical constraints

As previously discussed, the main characteristic feature of the Aegean subduction-arc system is the vertical superposition of three of its main components: a) active volcanic centers at the surface, b) a major low velocity, relatively flat body (fig. 7) below them, at a depth of 60 to 90 km within the overriding mantle wedge and, c) an 110 to 140 km depth segment of the subducting slab which is characterized by lower seismicity in comparison to

the shallower and deeper segments of the same slab (see figs 2, 3 and 7). This vertical superposition probably implies genetic links, since the presence of volcanoes above the low velocity body shows that the latter is most likely the main magma reservoir from which other higher lying magmatic chambers and finally the volcanoes themselves are periodically feeded with magma. However, the presence of the intermediate segment of lower seismicity in the subducted slab, straight below the main magma reservoir, is not easily understood and needs further explanation.

We propose that the critical factor determining the distance from the trench, the depth and the vertical arrangement of the three previous components is the presence of the geophysically observable location of the partial melting zone within the overriding mantle wedge, between the low seismicity segment below and the main magma reservoir above. This location is mainly determined by the subduction rate, the thermal state of the subducting slab, and the thermal structure of the overriding wedge. A partial melting front is actually forming when and where the hydrous fluids ascending from the down-going and dehydrating slab cross the wet mantle lherzolite solidus within the overriding mantle wedge. Further up-slab any watery fluids that were gradually released from the descending slab are either kept in the pores between the mineral grains sustaining a high pore fluid pressure or were stabilized in the overriding mantle in hydrous phases such as serpentine, phlogopite or amphiboles.

Within the overriding mantle wedge the partial melting front (to be imagined as a nearly completely solid mantle peridotite with only a small fraction of melt present as droplets and thin films round the mineral grains) is in fact a demanding water sink. The watery fluids released from the dehydrating slab below are therefore actively driven away from the zone of dehydration and are streaming up via interconnected tiny channels along grain boundaries towards the melting front above, leaving behind a far less hydrated residual. Any free water left in the zone of dehydration is probably also consumed in the partial melting of metasediments that might have been driven at this depth; such melts transport also upwards, reach the melting front and mix with the mantle derived melts. The mixed melts, being less dense than the surrounding minerals, migrate upwards and are collected in the main magma reservoir (the 60 to 90 km depth flat low velocity zone).

The dehydration of the upper part of the subducted slab below the melting front may be not complete. It can leave some hydrous minerals that can sustain high pressures in the metabasites of the oceanic crust. However, the removal of all the available free water will drop considerably the pore fluid pressure within the upper part of the slab at a level far below that necessary to compensate the existing high confining pressure. This may well explain the 110 to 140 km depth low seismicity segment of the down-going slab. Also, the resulted densification of this part of the slab can cause an increase in the subduction angle, a feature identified in the subducting Mediterranean oceanic slab from both tomographic results and the Benioff zone (figure 2 and 7, as well as results from Papazachos et al. (2000).

Further dehydration within the subducted slab, probably driven to completeness, will start again when the remaining high-pressure hydrous phases will no longer be stable under the conditions prevailing at greater depths (more than 140 km). The relatively little water released during this second dehydration stage is less likely to find its way to the previous or form a new zone of partial melting due to removal of solidus to higher temperatures and will probably only rise the pore fluid pressure.

It should be noted that existing geochemical data (Zellmer et al. 2000) are in accordance with the above proposed model, since they show that in the generation of at least the Santorini magma three components are involved: mantle wedge, sediment melts and slab derived fluids. Unfortunately, there are no available data on the thermal structure of either the subducting slab or the mantle wedge above it. However, the thermal structure of the subducting slab is mainly depended on the subduction rate, which can be inferred from the convergence rate between Africa and Europe, considering velocities ranging between 1 cm/yr and 5 cm/yr, with the velocity of 3-3.5cm/yr as a realistic estimate (e.g. Papazachos, 1999).

Using v=1 cm/yr, v=5 cm/yr and v=3cm/yr, a length scale (L) of 40 km (~one-half the thickness of the oceanic lithosphere) and a thermal diffusivity (κ) of 1mm^2/s, from the equation $P_e = (v \cdot L)/\kappa$ the three corresponding Peclet numbers (the lower, the higher and a

more probable intermediate one) are 13, 63 and 38, all greater than one. Thus, the advection of heat along with the subducting slab should occur at a much faster rate than the conduction of heat into the subducting slab. The thermal structure of the subducting slab must therefore feature strong depression of the isotherms. Additional factors farther depressing the isotherms are the endothermic intermediate metamorphic reactions, especially the devolatilization ones, and the partial melting of the metasediments. Factors opposing such a depression are the shear heating at the interface between the subducted slab and the overriding lithosphere and the radiogenic heat produced within the subducting sediments.

Since the thermal depression and the resulted inversion of the isotherms near the boundary between the subducted slab and the mantle wedge above it is a necessary prerequisite for melting to occur in the overriding mantle wedge and for the consequent expression of volcanic activity on the surface, we suggest that the depression and inversion of the isotherms characterizing most subduction zones (Anderson et al., 1978, 1980; Furlong et al., 1982) also exist in the Aegean subduction system. Shear heating and radiogenic heat production, therefore must not play a significant role in the case of the Aegean subduction. Given the large amount of sediments that are driven into the trench, a low radiogenic heat production may appear strange; however, due to the thin skin tectonic regime in the eastern Mediterranean (Kastens, 1991) large parts of these sediments may be detached from the slab and may not follow it at great depths.

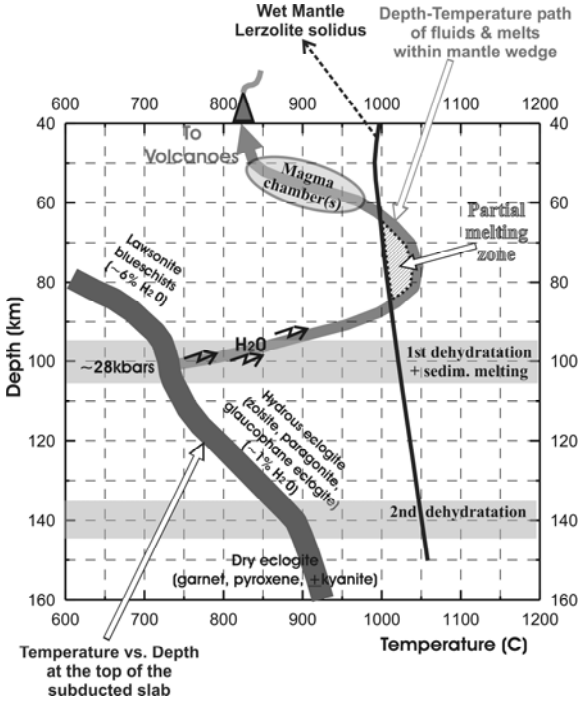

Fig. 8. Schematic depth-temperature diagram and corresponding geochemical information for the top part of the subducted slab and the depth-temperature path of fluids and melts derived from slab dehydration (see text for explanation).

We cannot go further deducing from the little available data more details for the thermal structure beneath the Aegean arc system. Nevertheless, we can make the realistic assumption that at 100 to 110 km depth, where we suggested that drastic dehydration of the basic oceanic rocks and partial melting of the subducted sediments should occur, the temperature in the upper part of the subducting slab should have reached ~700˚ C (fig. 8). The corresponding lithostatic pressure (assuming a column of 20 km of granite and 70 km of peridotite) should be there ~28 kbars (2.8 GPa). These conditions suggest a steep steady state geotherm within the upper part of the subducted slab, which will probably pass through the

zeolite, lawsonite-chlorite and lawsonite-blueshist facies, before entering the eclogite facies at pressures higher than 20 Gpa corresponding to depths more than 70 km (see for example Peacock, 1993, fig 2).

Taking into account that delays in the completeness of mineral reactions and metastable preservation of metamorphic assemblages is the rule rather than the exception for rocks following steep geotherms, we can make a realistic suggestion that at about 100 to 110 km lawsonite-glaucophane metabasites of the oceanic crust are converted to glaucophane bearing eclogites, at the same time that partial melting of metasediments is taking place. This conversion will drop the water content of the oceanic metabasites from nearly 6% to less than 1%, freeing thus significant amounts of water that escape up to the melting front within in the overriding mantle wedge. The not completely dry eclogite formed may contain zoisite, paragonitic mica and glaucophane, along with garnet and pyroxene. These minerals remain stable until the increasing temperature and pressure further deeper will gradually destabilize them, freeing again small amounts of water and leaving behind a completely dry garnet-pyroxene eclogite. This second dehydration may just increase the pore fluid pressure allowing seismicity to appear again (for depths > 130-140 km). It should be noted that the possibility that hydrous phases within the subducted oceanic crust may persist at depths much larger than 100 km, even down to 250 km, is not unlikely; such a possibility is supported by theoretical and geophysical data (Peacock, 1993; Abers, 2000).

A Synthetic Model for the Southern Aegean subduction

Data presented in the present work combined with already published information can be used to propose a synthetic model for the deep active tectonic structure of the southern Aegean. Such a model, in addition to information on the converging lithospheric plates, should also include information on the location and size of the primary magma zone. Such information and knowledge on the genesis of primary magma in island arcs (Abers, 2000; Yamasaki and Seno, 2003, among others) can be used to propose a reasonable hypothesis on the way that primary magma is generated in the Hellenic arc.

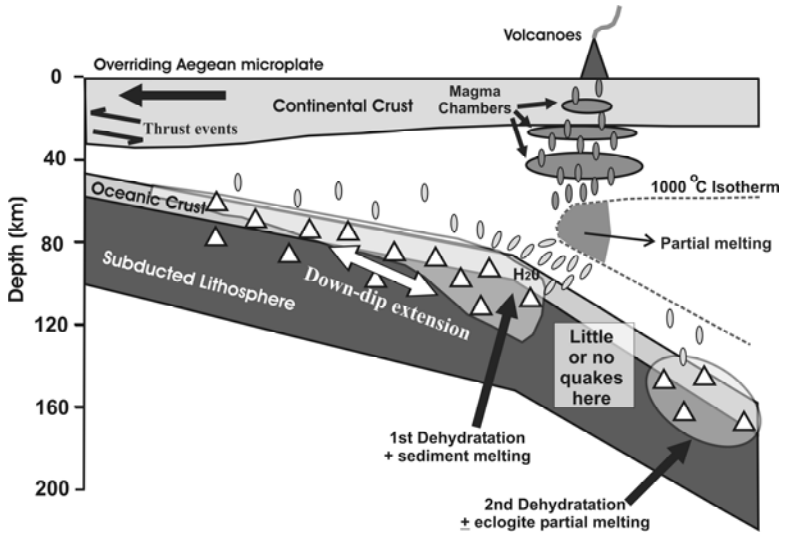

Fig. 9. A synthetic model for the active tectonic structure of southern Aegean.

A schematic synthetic model is shown in figure (9), which shows a vertical profile of the deep tectonic structure of the Hellenic arc in an ~SSW – NNE direction (approximately normal to the arc). The thickness of the descending eastern Mediterranean slab (front part of the African plate) is taken equal to 70-90km, which is the thickness of the layers above the top of the low shear wave velocity layer, estimated from phase velocity of Rayleigh waves (Papazachos, 1969), as well as tomographic results (Papazachos and Nolet, 1997). The thickness of the crustal oceanic layer of the slab has been set to ~7km by wide aperture

seismic data (Bohnhoff et al., 2002). The thickness of the overriding Aegean crust varies along the profile, while its lithospheric thickness is considered to be of the order of 50km in the volcanic arc area (Papazachos, 1969; Makris, 1976,1978; Papazachos and Nolet, 1997; Bohnhoff et al., 2002; Karagianni et al., 2002). This is also supported by the observations that intermediate depth earthquakes ($h \geq 60$km) under the concave part of the arc are generated by down – dip tension (fig. 5), while shallow earthquakes ($h < 60$km) in the convex part of arc are generated by thrust faulting, as it is expected if the interaction between the two lithospheres occurs at a depth of about 40-50km. Considering that the mean thickness of the crust in the continental slab of southern Aegean is about 20-25km (Makris, 1976; Bohnhoff et al., 2002), the crust and lithospheric mantle of the overriding southern Aegean slab have similar thickness.

The eastern Mediterranean lithosphere moves to the north with a velocity of 5-10mm/yr with respect to Europe (McClusky et al., 2000), while the southern Aegean lithosphere moves southwestwards and overrides the Mediterranean lithosphere with a velocity of 30mm/yr (Papazachos, 1999). Hence, the subduction of the eastern Mediterranean slab with respect to the Aegean lithosphere should occur at a maximum rate of 4cm/yr in an NNE direction.

The vertical dimension of the primary magma zone can be considered equal to the vertical dimension of the low velocity layer under the volcanic arc as this dimension is derived by seismic tomography, that is, between 60km and 90km. The extent of this zone normal to the arc can be also considered to be defined by the distribution of the vertical projections of the five volcanic centers. The minimum and maximum distance of these volcanic centers from the isodepth of 100km is 10km (Sousaki) and 90km (Santorini), respectively, that is, the horizontal dimension of the primary magma zone normal to the arc is of the order of 80km, similar to what is found by the tomographic results (e.g. fig 7.)

Figure (9) shows that the zone of primary magma generation is just above the low seismicity part of the subducted oceanic crust. Based on this observation we may conclude that its low seismicity part of the oceanic crust is dehydrated at depths less than 110km and the released water contributes to the formation of primary magma. Information on trace element and isotopic data for the Santorini volcano supports the idea that the sources of magma generation in the Hellenic volcanic arc is the subducted oceanic crust and the mantle wedge between the two slabs (Zellmer et al., 2000).

The generation of intermediate depth earthquakes at the shallow part (60 – 110km) of the Benioff zone in south Aegean is convincingly explained by the hypothesis of dehydration embrittlement of the subducted slab in these depths. For the generation of earthquakes at the deeper part (140 – 180km) of these zone several explanations have been proposed worldwide (e.g. Wiens, 2001). It is possible that earthquakes at these depths are also generated by second dehydration embrittlement of basalt because calculations of seismic wave velocities show that the oceanic crust remains distinct to these depths (Abers, 2000). The second possibility is that earthquakes at these depths are generated by dehydration embrittlement of serpentine in case that the dipping slab is of cold type, because in such case the lower part of the dehydration loci of serpentine penetrates the lower seismically active part of the subducted slab (Yamasaki and Seno, 2003). For the southern Aegean subduction we propose that the second dehydration embrittlement of hydrous eclogite-basalt is the most locigal explanation for this seismicity, given the relatively young age and possibly high temperature of the southern Aegean subduction.

Conclusions and Discussion

The Mediterranean slab, with a thickness of about 80km and an oceanic crust of 7km, dips under the Aegean microplate at a mean angle of 25^{o}. The seismically active part of the upper layer of this slab (with earthquakes of $M \geq 4.0$) reaches up to a depth of 180km, but at depths 110 – 140km this layer is of relatively low seismicity due probably to its higher temperature. Earthquakes in the shallow part (60 – 110km) of this dipping Benioff zone are generated by down – dip tension, while maximum compression is horizontal and parallel to the Hellenic arc. Strong evidence is presented that the cause of intermediate depth

earthquakes in the shallow part of the Benioff zone of southern Aegean is the dehydration embrittlement of basalt while the earthquakes in the lower part of this zone are caused in the same way or are caused by a second similar dehydration embrittlement of hydrous eclogite.

Shallow earthquakes in the zone of convergence (Hellenic trench) of the eastern Mediterranean and Aegean lithospheres are generated by low dip angle thrust faulting trending NW – SE and dipping NE. Shallow earthquakes in the southern Aegean volcanic arc are generated by normal faulting trending in an about NE – SW direction.

The occurrence under the volcanic arc of both the low velocity mantle layer, at depths of 60 – 90km and of the low seismicity dipping oceanic crust, at depths of 110 – 140km, indicates that the primary magma in southern Aegean is located in the asthenospheric wedge between the descending Mediterranean and the overriding Aegean microplates under the volcanic arc, in agreement with geochemical data.

The available data do not allow to test the hypothesis whether there are two almost parallel Benioff zones in southern Aegean, as it occurs in other arcs (e.g.Yamazaki and Seno, 2003). We cannot, for example, exclude the possibility that earthquakes with focal depths 130 – 180km belong to a different zone than those at depths 60 – 120km. If this is the case, the shallower seismic zone is due to dehydration embrittlement of basalt and the lower seismic zone to dehydration embrittlement of hydrous eclogite. However, the problem needs further examination by the use of additional new data which will help to clarify the geometrical and geophysical constraints of the southern Aegean subduction.

Acknowledgements

This work has been funded by the e-Ruption project (contract EVR1-2001-00024).

References

Abers, G.A., 2000. Hydrated subducted crust at 100-250Km depth. Earth Planet. Scie. Lett., 176: 323-330.

Anderson, R. N., DeLong, S. E. and Schwarz, W. M., 1978. Thermal model for subduction with dehydration in the downgoing slab. J. Geol., 86: 731-739.

Anderson, R. N., DeLong, S. E. and Schwarz, W. M., 1980. Dehydration, asthenospheric convection and seismicity in subduction zones. J. Geol., 88: 445-451.

Bohnhoff, M., Makris, J., Papanikolaou, D. and Stavrakakis, G., 2002. Crustal investigation of the Hellenic subduction zone using wide aperture seismic data. Tectonophysics, 343: 239-262.

Comninakis, P.E. and Papazachos, B.C., 1980. Space and time distribution of the intermediate focal depth earthquakes in the Hellenic arc. Tectonophysics, 70: 35-47.

Drakatos, G. and Drakopoulos J., 1991. 3-D velocity structure beneath the crust and upper mantle of the Aegean sea region. Pure Appl. Geophys., 135: 401-420.

Fytikas, M., Innocenti, F., Manetti, P., Mazzuoli, R., Pecerillo A. and Villari L., 1985. Tertiary to Quaternary evolution of the volcanism in the Aegean region. In: J.F. Dixon and A.H.F. Robertson (Editors), The Geological Evolution of the Eastern Mediterranean. Blackwell Publ., Oxford, pp. 848.

Furlong, K. P., Chapman, D. S. and Alfeld, P. W., 1982. Thermal modeling of the geometry of subduction with implications for the tectonics of the overriding plate. J. Geophys. Res., 87: 1786-1802.

Georgalas, G.C., 1962. Active volcanoes in the world including solfatara fields. Intern. Volcan. Assoc., 12: 1-40.

Hatzfeld, D., Pedotti, G., Hatzidimitriou, P., Panagiotopoulos, D.G., Scordilis, M., Drakopoulos, J., Markopoulos, K., Delibasis, N., Latoussakis, J., Baskoutas, J. and Frogneua, M., 1989. The Hellenic subduction beneath the Peloponnese: first results of a mivroearthquake study. Earth Planet. Sci. Lett., 93: 283-291.

Jackson, J., 1994. Active tectonics of the Aegean region. Annu. Rev. Earth Planet Sci., 22: 239-271.

Karagianni, E.E., Panagiotopoulos, D.G., Panza, G.F., Suhadolc, P., Papazachos, C.B., Papazachos, B.C., Kiratzi, A., Hatzfeld, D., Makropoulos, K., Priestly, K. and Vuan, A., 2002. Tectonophysics, 358: 187-209.

Kastens, K., 1991. Rate of outward grouth of the Mediterranean Ridge accretionary complex. Tectonophysics, 199: 25-50.

Kiratzi, A.A. and Langston, Ch. A., 1989. Estimation of earthquake source parameters of the May 4, 1972 event of the Hellenic arc by the inversion of waveform data. Physics Earth and Planet. Inter., 57: 225-232.

Kiratzi, A.A. and Papazachos, C.B., 1995. Active seismic deformation in the southern Aegean Benioff zone. J. Geodynamics, 19: 65-78.

LePichon, X., Chamot-Rooke, N., Lallemant, S., Noomen, R. and Veis, G., 1995. Geodetic determination of the kinematics of central Greece with respect to Europe: implication for eastern Mediterranean tectonics. J. Geophys. Res., 100: 12675-12690.

Ligdas, C.N., Main, I.G. and Adams, R.D., 1990. 3-D structure of the lithosphere in the Aegean sea region. Geophys. J. Int., 102: 219-229.

Makris, J., 1976. A dynamic model of the Hellenic arc deduced from geophysical data. Tectonophysics, 36: 339-346.

Makris, J., 1978.The crust and upper mantle of the Aegean region from deep seismic soundings. Tectonophysics, 46: 269-284.

McClusky, S., Balassanian, S., Barka, A., Demir, C., Ergintav, S., Georgiev, I., Gurkan, O., Hamburger, M., Hurst, K., Kahle, H., Kastens, K., Kekelidze, G., King, R., Kotzev, V., Lenk, O., Mahmoud, S., Mishin, A., Nadariya, M., Ouzounis, A., Paradissis, D., Peter, Y., Prilepin, M., Reilinger, R., Santli, I., Seeger, H., Tealed, A., Toksoz, M.,N. and Veis, G., 2000.Global Positioning System constraints on plate kinematics and dynamics in the eastern Mediterranean and Caucasus. J. Geophys. Res., 105: 5695-5719.

McKenzie, D.P., 1970. The plate tectonics of the Mediterranean region. Nature, 226: 239-243.

McKenzie, D.P., 1972. Active tectonics of the Mediterranean region. Geophys. J.R. Astr. Soc., 30: 109-185.

McKenzie, D.P., 1978. Active tectonics of the Alpine-Himalayan belt: the Aegean sea and surrounding regions. Geophys. J.R. Astr. Soc., 55: 217-254.

Papadimitriou, E.E., 1993. Focal mechanism along the convex side of the Hellenic arc and its tectonic significance. Bull. Geof. Teor. Appl., 35: 401-426.

Papazachos, B.C., 1969. Phase velocities of Rayleigh waves in southeastern Europe and eastern Mediterranean sea. Pure Appl. Geophys., 75: 47-55.

Papazachos, B.C. and Comninakis, P.E., 1969/1970. Geophysical features of the Greek island arc and eastern Mediterranean ridge. Final Proc. Seances de la Conference Reunie a Madrid , Madrid, Spain, pp. 74-75.

Papazachos, B.C. and Comninakis, P.E., 1971. Geophysical and tectonic features of the Aegean arc. J. Geophys. Res., 76: 8517-8533.

Papazachos, B.C. and Panagiotopoulos, D.G., 1993. Normal faults associated with volcanic activity and deep rupture zones in the southern Aegean volcanic arc. Tectonophysics, 220: 301-308.

Papazachos, B.C., Karakostas, V.G., Papazachos, C.B. and Scordilis, E.M., 2000. The geometry of the Wadati-Benioff zone and lithospheric kinematics in the Hellenic arc. Tectonophysics, 319: 275-300.

Papazachos, B.C. and Papazachou, C.B., 2003. The earthquakes of Greece. Ziti, Thessaloniki.

Papazachos, B.C., Comninakis, P.E., Karakaisis, G.F., Karakostas, B.G., Papaioannou, Ch.A., Papazachos, C.B., Scordilis E.M., 2003. A catalogue of earthquakes in greece and surrounding area for the period 550BC-2002. Publication, Geophys. Lab. Univ. Thessaloniki, Thessaloniki, Greece.

Papazachos, C.B., 1999. Seismological and GPS evidence for the Aegean – Anatolia interaction. Geophys. Res. Lett., 26: 2653-2656.

Papazachos, C.B. and Kiratzi, A.A., 1992. A formulation for reliable estimation of active crustal deformation and an application to central Greece. Geophys. J. Int., 111: 424-432.

Papazachos, C.B., Hatzidimitriou, P.M., Panagiotopoulos, D.G. and Tsokas, G.N., 1995. Tomography of the crust and upper mantle in southeast Europe. J. Geophys. Res., 100: 12405-12422.

Papazachos C.B. and Nolet, G.P., 1997. P and S deep velocity structure of the Hellenic area obtained by robust nonlinear inversion of travel times. J. Geophys. Res., 102: 8349-8367.

Peacock, S. M., 1993. The importance of blueschist-eclogite dehydration reactions in subducting oceanic crust. Geol. Soc. America Bull., 105: 684-694.

Reilinger, R. E., McClusky, S. C., Oral, M. B., King, R. W., Toksoz, M. N., Barka, A. A., Kinik, I., Lenk, 0. and Sanli, I., 1997. Global Positioning System measurements of present-day crustal movements in the Arabia-Africa-Eurasia plate collision zone. J. Geophys. Res., 102: 9983-9999.

Spakman, W., 1986. Subduction beneath Eurasia in connection with the Mesozoic Tethys. Geol. Mijnb., 65: 145-153.

Spakman, W., Wortel, M. J.R. and Vlaar, N.J., 1988. The Hellenic subdustion zone: a tomographic image and its dynamic implication. Geophys. Res. Let., 15: 60-63.

Straub, Ch. and Kahle, H.G., 1994. Global positioning system estimated in the Marmara sea region, northwestern Anatolia. Earth Planet Sci. Lett., 121: 495-502.

Taymaz, T., Jackson, J. and Westaway, R., 1990. Earthquake mechanisms in the Hellenic trench near Crete. Geophys. J. Int., 102: 695-731.

Wiens, D.A., 2001. Seismological constrains on mechanism of deep earthquakes: temperature dependence of deep earthquake source properties. Phys. Earth Planet. Inter., 127: 145-163.

Yamasaki, T. and Seno, T., 2003. Double seismic zone and dehydration embrittlement of the subtucting slab. J. Geophys. Res., 108: 2212-2233.

Zellmer, G., Turner, S. and Hawkesworth, C., 2000. Timescales of destructive plate margin magmatism: new insights from Santorini, Aegean volcanic arc. Earth Planet. Scie. Lett., 174: 265-281.